New Method for Systems and Cost Analysis of Human Mars Entry Vehicles

Paul D. Friz* and Jamshid A. Samareh†
NASA Langley Research Center, Hampton, VA, 23681, USA

Serhat Hosder‡
Missouri University of Science and Technology, Rolla, MO 65401, USA

Cost is one of the biggest obstacles to sending humans to Mars. However, spacecraft costs are typically not estimated until after the preliminary vehicle and mission concepts have been designed. By automating the cost estimation process, the effect of any change in vehicle or mission design on the mission cost can be determined more efficiently. This paper describes an extension to the tool SAPE (Systems Analysis for Planetary Entry, Descent, and Landing). This extension integrates the cost modeling software SEER-H (System Estimation and Evaluation of Resources-Hardware) with a number of systems analysis tools. This new method is used to analyze several tradespaces of a HIAD (Hypersonic Inflatable Aerodynamic Decelerator) entry vehicle for human Mars missions. Key findings include quantifying the impacts of ballistic coefficient, main engine specific impulse, and thrust-to-weight ratio on the overall cost of the vehicle, and how the payload per lander and number of landers affects the cost of a campaign to Mars.

Nomenclature

AC	=	Aerocapture
CBE	=	Current Best Estimate
CDF	=	Cumulative Distribution Function
CER	=	Cost Estimating Relationship
CI	=	Confidence Interval
CH4	=	Methane
ConOps	=	Concept of Operations
EDL	=	Entry, Descent, and Landing
EXAMINE	=	Exploration Architecture Model for the IN-space and Earth-to-orbit modeling

*Student Trainee (Engineering), Systems Analysis and Concepts Directorate, AIAA Student Member.
†Aerospace Engineer, Systems Analysis and Concepts Directorate, Associate Fellow AIAA.
‡Associate Professor of Aerospace Engineering, Department of Mechanical & Aerospace Engineering, Associate Fellow AIAA.

FEA	=	Finite Element Analysis
HARA	=	High-temperature Aerothermodynamic RAdiation
HIAD	=	Hypersonic Inflatable Aerodynamic Decelerator
LAURA	=	Langley Aerothermodynamic Upwind Relaxation Algorithm
LOX	=	Liquid Oxygen
MAV	=	Mars Assent Vehicle
MDM	=	Mars Descent Module
MEL	=	Master Equipment List
MSL	=	Mars Science Laboratory
PDF	=	Probability Distribution Function
Post II	=	Program to Optimize Simulated Trajectories II
RCS	=	Reaction Control System
SAPE	=	Systems Analysis for Planetary EDL
SAPE-C	=	Systems Analysis for Planetary EDL-Cost
SEER-H	=	System Estimation and Evaluation of Resources-Hardware
t	=	Metric Ton
TCS	=	Thermal Control System
TMI	=	Trans-Mars Injection
TPS	=	Thermal Protection System

I. Introduction

ONE of the biggest obstacles for getting humans to Mars is cost[1–3]. When designing a new spacecraft, vehicle concepts are formulated based on a data-driven and physics-based systems analysis. Meanwhile, design decisions intended to reduce cost are often based on the faulty assumption that lower mass equates to lower cost. Cost is usually modeled in a fairly static fashion; typically, a cost estimate is produced for a single conceptual design after a trade study is completed. Thus, all other candidate designs in the tradespace are ignored. A reason for this is that the user interfaces for cost estimating models make cost tradespace exploration very time consuming by requiring users to manually change each input to the model.

Often technology development programs are funded because it is believed that they will reduce costs of future space missions. It is relatively easy to quantify how an improved technology or capability will reduce cost on a component level, but to quantify how that technology will affect the cost of a system requires a great amount of effort. For example, improved aerothermal models and knowledge of the Martian atmosphere will allow engineers to reduce the safety

margins on heatshield thickness. It is easy to model how this will reduce the cost of the heatshield but difficult to model how it will reduce the total cost of the entry system. Reduction in heatshield mass means less fuel is required to carry the lander to the surface, which in turn reduces the size of the tanks and supporting structures on the lander, reducing the cost further. Similarly, increasing the specific impulse of the descent engines will likely increase the mass and cost of the engines but will reduce the required fuel and tank size, decreasing the overall costs of the lander, but by how much? Is it a better investment to improve aerothermal models to reduce heatshield mass, or would the money be better spent improving engine technology? Would this answer change if the required payload was increased by 50% or if mission planners required a different trajectory? To answer these questions would require a massive effort using traditional cost modeling tools.

The present paper presents a novel approach to modeling cost for human Mars missions which bridges the gap between cost and systems analysis models. This tool should drastically reduce the time spent by cost estimators conducting trade studies allowing cost to be included in the systems analysis tradespace for entry vehicle design. This approach is implemented via a Python-based software tool known as System Analysis for Planetary EDL-Cost (SAPE-C). SAPE-C is an addition to the Python based tool SAPE developed by Samareh et al.[4][5] which is in itself an integration of many systems analysis tools. The primary goal of SAPE-C is to reduce the effort required by systems analysts in determining the impact that a new vehicle configuration, or improved technology will have on the overall cost of a system. This paper will introduce the tool SAPE-C, and will show the effects various improvements in technology or mission design parameters will have on the cost and cost uncertainty of a Hypersonic Inflatable Aerodynamic Decelerator (HIAD) entry vehicle designed to carry humans or cargo to the surface of Mars.

The following section describes the primary systems analysis tools that make up SAPE, SAPE-C, and the methods used to tie them together. Section III describes the concept of operations during the aerocapture and EDL phases of flight for the HIAD entry vehicle used in the present study. Section IV presents the results of using SAPE-C to analyze the cost of a HIAD entry vehicle. The tradespaces explored include: payload vs ballistic coefficient (Secs. IV.A, IV.B, and IV.C), payload vs specific impulse (Sec. IV.D), and payload vs thrust-to-weight ratio (Sec. IV.E). Section. IV.A varies the ballistic coefficient during aerocapture and EDL together while Secs. IV.B, and IV.C vary them independently. Section V demonstrates the uncertainty quantification capabilities of SAPE-C using the payload vs ballistic coefficient tradespace from Sec. IV.A as an example. Finally, Sec. VI summarizes the present work, provides concluding remarks, and discusses future work to be done to improve SAPE-C.

II. Methods: SAPE, SAPE-C and Associated Tools

Mars entry vehicles are very complex and highly coupled systems with many competing requirements and design variables. Changing the size or requirements of one component of the vehicle will affect the size and requirements of many other components of the entry vehicle. Understanding the tradespace of the design variables and the sensitivity

of the vehicle's performance parameters to those variables is critical to the design decision making process. Systems analysis and tradespace exploration provide a holistic view of a new vehicle or mission concept by enabling decision makers to gain a better understanding of how multiple design variables affect the vehicle as a whole. It is important that design decisions are made based on quantitative data and not on intuition. When done properly a systems analysis will use quantitative data to form verified models that show a systems response to a number of different design variables and quantify the uncertainty of the models. The traditional systems analysis process may take from several weeks to several years to complete. This can be significantly improved by automating and streamlining the analysis process. These improvements can also reduce the errors resulting from manual data transfer among discipline experts. The improved process will speed up the analysis and design activities such as tradespace studies, sensitivity analyses, uncertainty quantification, and vehicle optimization. However, automated systems analysis tools cannot replace the role of discipline experts, as their input is required to check the accuracy of both the inputs and outputs to the models.

The implementation of the systems analysis approach presented here is a modified version of the Systems Analysis for Planetary EDL (SAPE) tool. SAPE is a Python-based tool which combines a number of other software tools and vehicle analysis models, allowing it to provide analysis on entry vehicle geometry, trajectory, aerothermodynamics, thermal protection systems, and structure sizing[4][5]. SAPE provides an integrated environment so that a low-fidelity systems analysis and tradespace exploration can be performed in minutes, (not days or weeks) with sufficient hooks to perform high-fidelity analysis. SAPE has many capabilities, but for the purposes of this study it is used to quickly produce a Master Equipment List (MEL) and mass estimates of the vehicle's components. An exploded view of the HIAD entry vehicle analyzed in this work is shown in Fig. 1. This figure also shows which models within SAPE are used to size the different portions of the vehicle. SAPE contains a number of mass models for HIAD systems including flexible Thermal Protection System (TPS)[6], inflatable structure[7][8], inflation system[9], and rigid nose[10]. These models were created by consulting subject matter experts and using previous works. For aerothermal prediction, SAPE uses the data generated by LAURA (Langley Aerothermodynamic Upwind Relaxation Algorithm)[11] for the convective heating component and HARA (High-Temperature Aerothermodynamic RAdiation)[12–14] for the radiative heating component. In addition to the previously mentioned models, SAPE also integrates the vehicle sizing tool EXAMINE (Exploration Architecture Model for the IN-space and Earth-to-orbit modeling)[15] for sizing the Mars Descent Module (MDM), and POST II (Program to Optimize Simulated Trajectories II)[16] for modeling the trajectories and determining fuel burn.

SAPE-C is a separate Python code, which integrates SAPE and the parametric cost modeling software tool SEER-H (System Estimation and Evaluation of Resources-Hardware). This allows the user to explore large tradespaces in vehicle design and see how any variable affects the cost of the vehicle hardware. A flow chart showing a simplification of the SAPE/SAPE-C algorithm is shown in Fig 2. The SAPE/SAPE-C algorithm works as follows. First the user defines the initial orbit of the spacecraft and its design parameters such as payload, ballistic coefficient, and specific

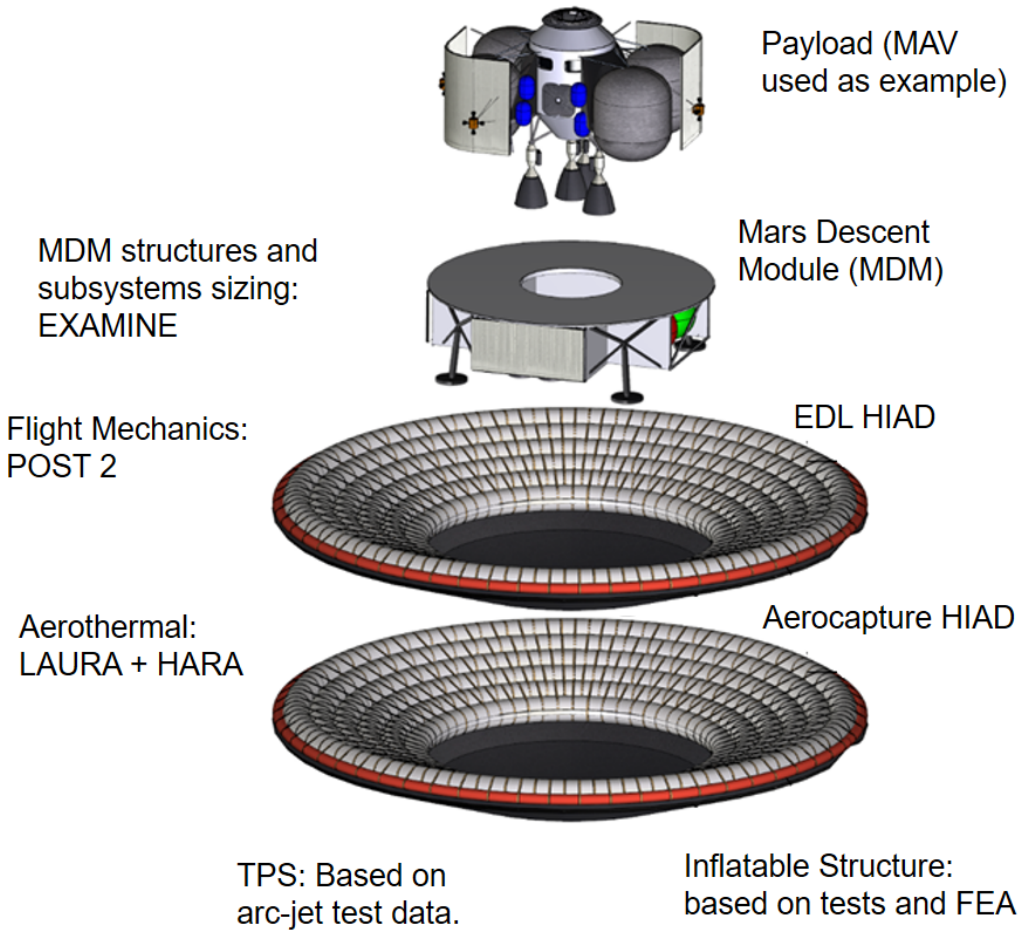

Fig. 1 Exploded view of HIAD entry vehicle and system models used by SAPE.

impulse. An initial mass estimate of the vehicle as it arrives at Mars is then used to seed the SAPE algorithm. These initial estimates and design parameters are written into an existing POST II input file. POST II then calculates the required delta-V/propellant burned from the simulated trajectory. The trajectory information is used in conjunction with LAURA and HARA to estimate the radiative and convective heat fluxes that the TPS must withstand. SAPE then estimates the required thickness of the HIAD TPS. The HIAD TPS thickness is used to estimate the mass of the HIAD structures. EXAMINE then uses the estimated mass of the HIADs and required propellants to estimate the masses all the components of the structures, thermal, propulsion, and power subsystems on the MDM. The initial arrival mass minus the sum of the masses of the MDM, HIADs and propellant is equal to the available payload mass. If the available payload mass is significantly different from the required payload mass, then an updated mass estimate will be input to POST again and the vehicle sizing process will be repeated until the algorithm converges. The method used to update the vehicle mass and other properties is similar the Gauss-Seidel method. Once convergence is achieved, the mass estimates of all the vehicle components are used by SAPE-C to generate a SEER command file that is used to estimate

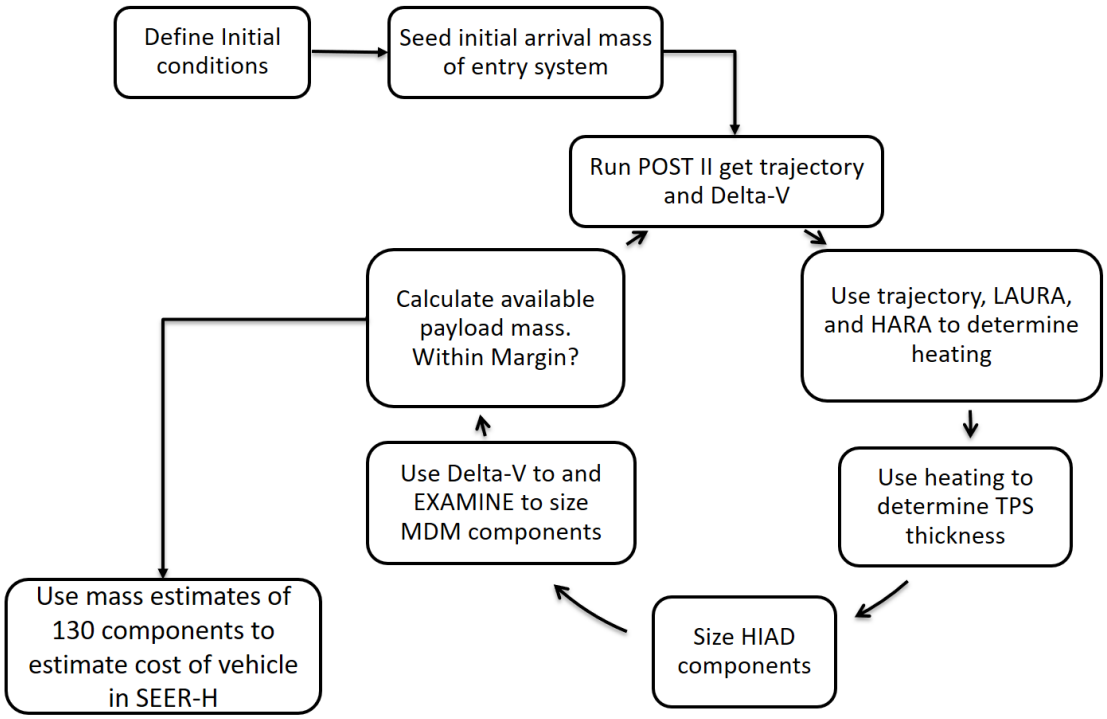

Fig. 2 SAPE/SAPE-C Algorithm.

the cost of the vehicle.

The three primary tools used by SAPE-C—POST II, EXAMINE, and SEER-H—are briefly described in the following sections.

A. Program to Optimize Simulated Trajectories II (POST II)

The Program to Optimize Simulated Trajectories II (POST II) software is used by SAPE for flight mechanics[16]. The Post II software is a generalized point mass, discrete parameter targeting and optimization program that has been used extensively in past Mars missions such as the Mars Exploration Rovers and Mars Science Laboratory. For this study, candidate configurations were evaluated by modeling both aerocapture and EDL trajectories in Post II. These simulations used standard Mars gravity, terrain and planet models, and the Martian atmosphere was modeled using the 2010 Mars Global Reference Atmospheric Model (Mars-GRAM 2010). An aerodynamic database for a 70° sphere cone HIAD was incorporated into the Post II simulation, and the database consisted of axial and normal force coefficient tables for a range of Mach and angle-of-attack values. EXAMINE determines the mass of the MDM and SAPE determines the mass of the HIADs, which are summed together with the payload and propellant masses to determine the TMI mass. The TMI mass is then used as an input into POST II, which updates the estimate of the propellant mass used by EXAMINE.

B. Exploration Architecture Model for the IN-space and Earth-to-orbit modeling (EXAMINE)

Exploration Architecture Model for the IN-space and Earth-to-orbit modeling (EXAMINE) developed by D.R. Komar is an Excel-based tool for sizing spacecraft and launch vehicles[15]. In SAPE it is used to generate a Master Equipment List (MEL) of all components in the Mars Descent Module (MDM). The MDM is then broken up into the following lander subsystems: Structures, Main Propulsion System (MPS), Reaction Control System (RCS), Power, and Thermal Control System (TCS). EXAMINE models 41 individual components from these subsystems that are inputs to SEER. Some examples of these components include: landing legs, fuel tank structure, fuel tank spray on foam insulation, MPS fuel feed systems, helium pressurization storage system, solar arrays, radiators, etc. One of the primary inputs to EXAMINE is Delta-V, which determines how much fuel is required by the MPS and RCS during EDL.

C. System Estimation and Evaluation of Resources-Hardware (SEER-H)

System Estimation and Evaluation of Resources-Hardware (SEER-H) or simply SEER is a commercial parametric cost estimating tool developed by Galorath Inc. It is one of the standard tools used by NASA to estimate the costs of space missions for early planning or proposal phases. Galorath performed an internal validation study of SEER where it was used to predict the costs of 15 NASA space science missions. Galorath found that SEER's mean error in predicting mission cost was -1% with a standard deviation of 19%[17]. The first author performed an independent validation study of SEER and other parametric cost estimating tools in an attempt to verify Galorath's results[18]. The primary result of the SEER validation study was that when using SEER's uncertainty quantification capabilities 75% of the cases studied fell within SEER's 80% confidence interval*, thereby validating the predictions of SEER.

The backbone of SEER is its proprietary Cost Estimating Relationships (CERs) and associated database of cost history. To model the cost of a spacecraft in SEER, the user inputs "work elements" which correspond to different components of the spacecraft. For each "work element" the user chooses an "application" which sets the majority of the inputs for SEER's CERs. SEER's database contains hundreds of mechanical/structural "applications" for spacecraft components; examples include payload adapter, separation mechanism, space propulsion component, aerodynamic control surface, spacecraft antenna – dish, spacecraft harness, gimbal mechanism, etc. Mechanical/structural "applications" in SEER are modeled using mass, material composition, complexity of form, complexity of fit, construction process, amount of new design, design replication, certification level, and a number of other inputs. Electrical components are modeled using the number of printed circuit boards, number of discrete components per board, number of integrated circuits per board, clock speed, number of pins, percent new design, and a number of other inputs. If the user knows all these inputs they can potentially improve the accuracy of the estimate by inputting them into SEER. Otherwise, SEER will estimate the inputs using its database and the electronic "application" input by the user. If a spacecraft component does not have a matching "application" in SEER, the user can select an analogous technology and alter the inputs. For example, flexible

*SEER outputs project costs at probability levels in intervals of 10%. Thus 80% confidence intervals must be used as opposed to the more common 95% confidence interval.

TPS is not in SEER's database, and it was modeled as multi-layer insulation with adjustments to material composition, complexity of fit/form, and construction process.

For every input in SEER the user defines a "least," "likely," and "most" value corresponding to an optimistic, most likely, and pessimistic assumption for the input. Mass modeling in the present work assumed the "least" value was the Current Best Estimate (CBE), the "likely" value was the CBE plus the Mass Growth Allowance (MGA) and the "most" input was 30% more than the "likely" input. These assumptions are recommended in Galorath's SEER Space Guidance document[19]. Also, the NASA Jet Propulsion Laboratory's design principles document recommends that space missions carry a 30% mass margin above the MGA[20]. SEER models uncertainty by assigning each "work element" a distribution of possible costs in addition to a median cost. The least/likely/most inputs for each work element correspond to the lower bound, mode, and upper bound of a beta distribution. By default SEER uses the median value of each beta distribution as the input to its CERs. To model uncertainty SEER can also output a CDF, however, SEER only outputs the CDF in 10% increments from 10-90%. Thus, an 80% confidence interval instead of the more common 95% confidence interval is used in this study.

A baseline model of the lander including MDM, aerocapture HIAD, and EDL HIAD was created in SEER. The model was broken down by subsystems, which include: Structures, Main Propulsion System (MPS), Reaction Control System (RCS), Power, Avionics, Thermal Control System (TCS), Aerocapture HIAD, and EDL HIAD. In total 130 individual components of the lander were modeled in SEER including main engines, propellant tanks, fuel feed systems, radiators, solar panels, individual layers of HIAD TPS, antennas, and transponders, etc. Components from the Structures, MPS, RCS, Power, and TCS were modeled using mass estimates from EXAMINE. Avionics were modeled from the MEL produced by the Mars EDL Pathfinder study[21]. Note that the avionics cost estimate only includes the hardware cost and not any costs associated with developing the vehicle's software. The HIADs are modeled using output from SAPE. A cost and mass breakdown of the baseline lander design by subsystem can be seen in Fig. 3. While propellant makes up 37% of the landers mass, its cost is negligible compared to the hardware costs and is not included in the cost estimate. Note that while the mass of each subsystem is related to its cost, there is not a one-to-one correspondence between the mass breakdown and the cost breakdown. The Vehicle Systems Cost shown in Fig. 3a is the cost of project management, systems engineering, and integration assembly and test associated with the contractors building the vehicle. Any contractor award fees are not included in the estimate. Mission Systems Costs represents NASAs project management, systems engineering, and safety and mission assurance work.

Currently SAPE-C models how the cost of nearly every component of the entry vehicle changes. Some additional work remains to model how the cost of a small number of the components change, however, these components make up less than 10% of the total cost of the baseline vehicle. As a result cost estimates presented in this work for vehicles with payloads over 20 t will have their costs slightly underestimated while vehicles with payloads under 20 t will be slightly overestimated.

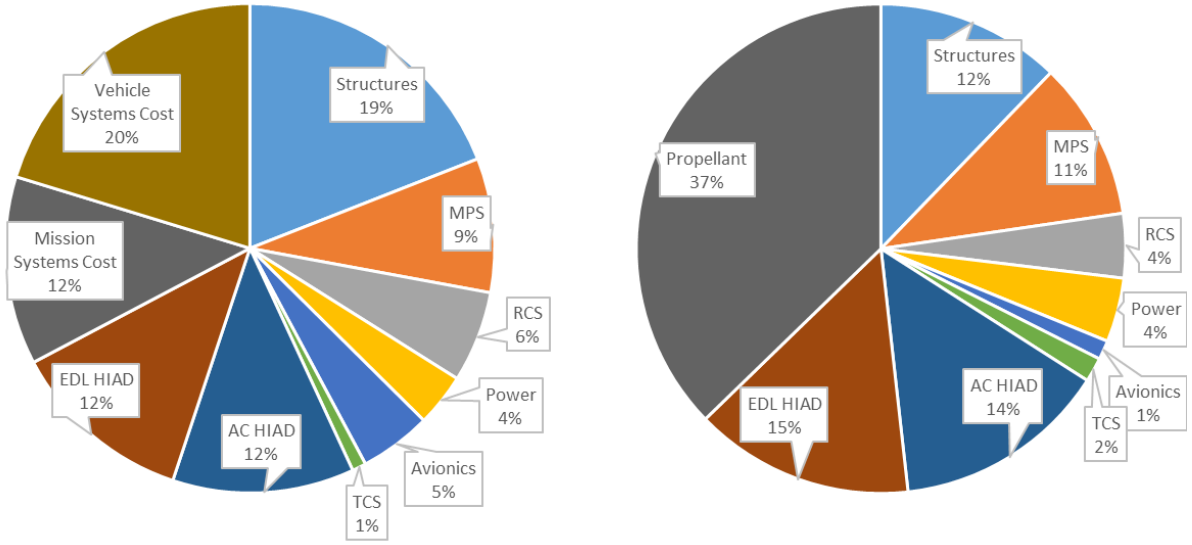

(a) Production Cost Breakdown. **(b) Mass Breakdown.**

Fig. 3 Production cost and mass breakdowns of baseline HIAD lander design.

III. EDL Concept of Operations

The concept of operations (ConOps) for this trade study is a lander spacecraft equipped with an aerocapture HIAD, EDL HIAD, descent stage or MDM, and payload. The lander is delivered to a Trans-Mars Injection (TMI) orbit by an in-space propulsion stage, which is not included in this analysis. After separating from the in-space propulsion stage, the lander approaches Mars with a hyperbolic velocity of 3,758 m/s and aerocaptures into a Mars one-solar day (1-Sol) parking orbit. After aerocapture the lander jettisons its aerocapture HIAD and loiters in orbit for up to a year. When the lander is needed on the surface, it makes a deorbit burn, deploys the EDL HIAD, and enters the Martian atmosphere. An artists conception of the entry phase can be seen in Fig. 4. In the hypersonic phase of entry, the lander uses trim tabs on the EDL HIAD and its CH4-LOX RCS for control. The lander takes advantage of atmospheric drag from its EDL HIAD to slow down to supersonic speeds. The landers ignites its eight CH4-LOX main engines at the proper time (typically at a speed of Mach 2-3) to reach to a vertical velocity of 2.5 m/s when it is 12.5 m above the surface. The lander then descends at a constant rate for 5 s until it lands safely. Once on Martian soil, the EDL HIAD will be retracted to allow for crew and cargo to be offloaded.

IV. Results

The tradespaces explored in this work include varying lander payload, ballistic coefficient of both aerocapture and EDL HIADs, engine specific impulse, and lander thrust-to-weight ratio. The results are primarily shown in contour plots with blue and red coloration, blue represents a lower cost, mass or other variables while red represents a higher

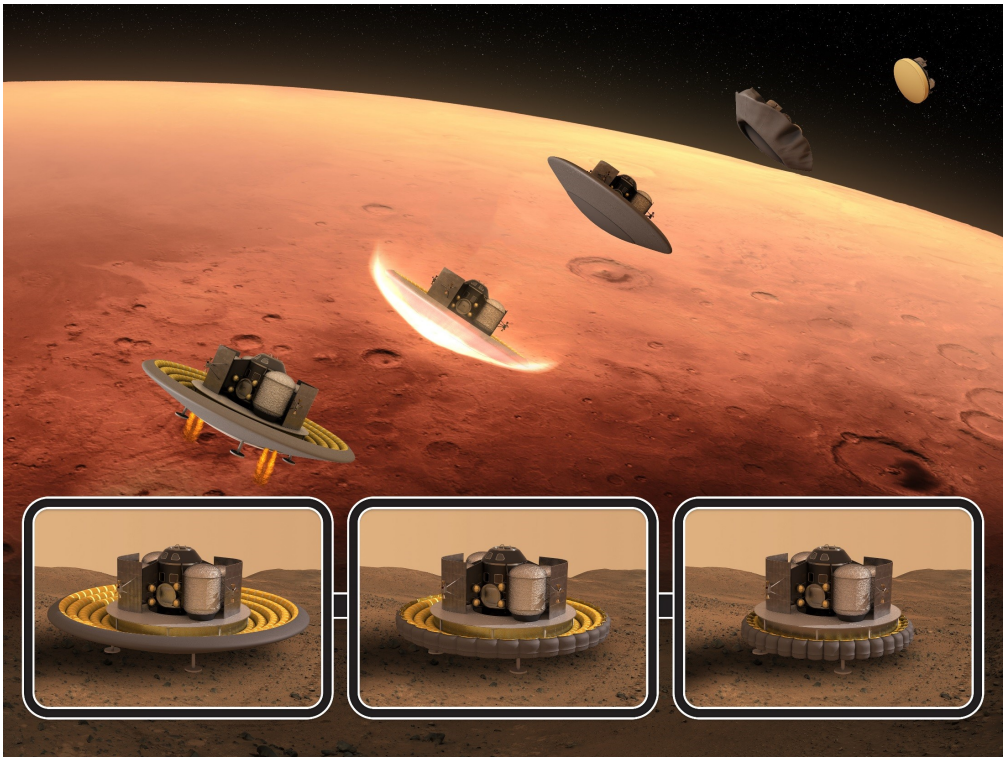

Fig. 4 Baseline EDL ConOps.

cost, mass or other variable. This work is not focused on determining the absolute cost of a campaign to Mars but rather how the relative cost changes as lander configuration and vehicle performance parameters are varied. Because of this and the uncertainty in the estimates of the exact costs, all costs presented have been normalized to the first unit production cost of the baseline lander design. The baseline lander has a payload capacity of 20 t, aerocapture and EDL HIADs with ballistic coefficients of 140 kg/m^2, main engine specific impulse of 360 s, and a thrust-to-weight ratio of 1.5. In the following sections the effect of each of these variables on lander cost, mass, as well as the total cost and mass of different Mars campaigns will be discussed. Section IV.A gives an in depth analysis of all the SAPE-C output as payload and ballistic coefficient are varied. This is followed by a detailed discussion on the effect of the payload per lander and thus, the number of landers on the total costs of a Mars campaign as well as the total TMI mass. Sections IV.B and IV.C isolate the effects that the ballistic coefficients of the aerocapture and EDL HIADs have on the total lander cost and TMI mass. Finally, Secs. IV.D and IV.E explore the effects that main engine specific impulse and thrust-to-weight ratio have on the total lander cost and TMI mass.

A. Introduction to SAPE-C Output:Payload vs. Ballistic Coefficient

This section gives a detailed description of much of the SAPE-C output, and demonstrates the capabilities of the tool using the payload vs. ballistic coefficient tradespace as an example. The remaining sections will not be as detailed or discuss all the plots presented here. However, all the plots presented for this tradespace will be available for the other

tradespaces in the Appendix.

A larger diameter HIAD creates a lower ballistic coefficient entry system. A lower ballistic coefficient allows more of the landers energy to be dissipated through drag and requires less propellant to be carried on the spacecraft. As a result of the reduced propellant requirements the tanks, thermal control systems, and structures all reduce in size, mass, and cost. However, at a point the additional mass and cost of a larger HIAD outweighs the mass and cost reductions from the other subsystems. In this tradespace the ballistic coefficient of both the AC and EDL HIADs are kept equal to each other and varied from 100 to 180 kg/m^2.

Figures 5a and 5b show the development cost and the production cost of the first unit for a lander with a given payload capacity and ballistic coefficient. All costs are normalized to the first unit production cost of the baseline lander design, which has a payload of 20 t and a ballistic coefficient of 140 kg/m^2. Development cost includes all costs associated with the design and test of a lander configuration including building and testing prototypes. First unit production cost includes all the costs associated with building the first flight unit. As each additional lander flight unit is produced, the workers building the lander gain experience, work more efficiently, and thus, the production cost decreases. In SEER this is modeled using Wrights Cumulative Average Model given by Eq. 1.

$$P_n = P_i N^b \tag{1}$$

The term P_i is the first unit production cost, N is the total number of units produced, P_n is the total cost to produce the N units, and b is a scaling factor between 0 and 1 that determines how much the cost is reduced for each additional unit produced. In SEER each component has its own b value determined by SEER's proprietary database and algorithms. Figure 5c shows the total cost to build five landers. The total cost is simply the sum of the development cost and the production cost to build five landers given by Eq 1. Note that for all configurations development cost is between 6.3 and 6.6 times the first unit production cost. For the b values given by SEER, this means eleven landers must be produced before the production costs are greater than the development costs. There is some variation, but this trend is relatively constant throughout this work.

In Figs. 5a, 5b, and 5c the primary cost driver is the payload carried by the lander. Moving from left to right along the x-axis, the payload increases and so does the cost. The ballistic coefficient is varied along the y-axis. For a lander with a given payload, increasing the ballistic coefficient from 100 kg/m^2 initially causes the costs decrease until they reach a minimum at a ballistic coefficient between 150 and 160 kg/m^2. Increasing the ballistic coefficient further causes the costs to increase again.

Figure 5d shows how the TMI (Trans-Mars Injection) mass changes with varying payload and ballistic coefficient. TMI mass is the mass of the lander with its payload when it is sent on its trajectory from Earth to Mars. Previous studies have focused on minimizing the TMI mass, assuming that minimizing TMI mass will minimize cost[2]. However,

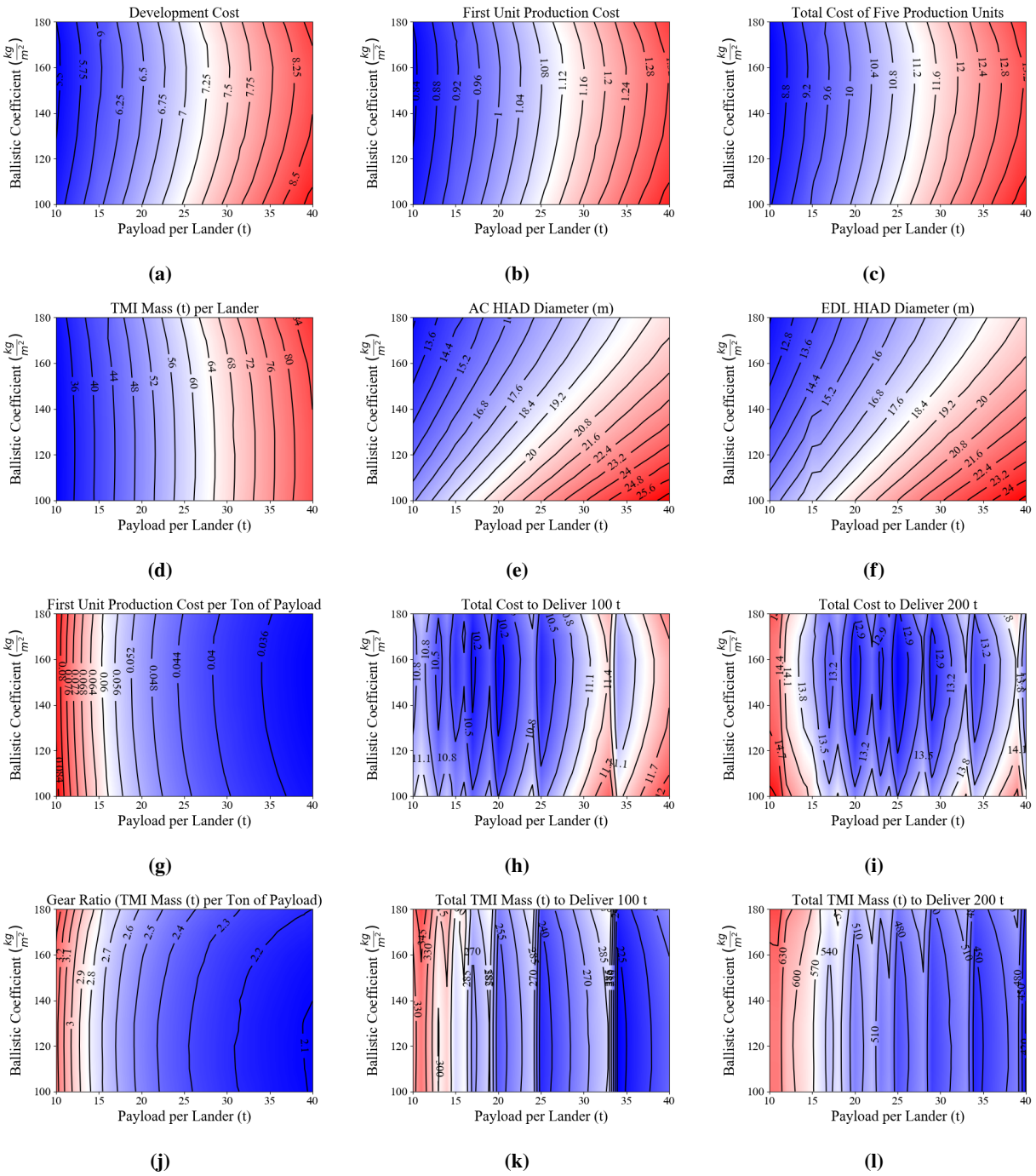

Fig. 5 Payload vs. Ballistic Coefficient Trades.

Figs. 5a, 5b, and 5c show that the lander hardware cost for a given payload is minimized at ballistic coefficients between 150 and 160 kg/m^2 while Fig. 5d shows the TMI mass is minimized for ballistic coefficients around 120 kg/m^2. For a lander with 20 t payload capacity decreasing the ballistic coefficient from 160 to 120 will decrease TMI mass by 1.73%, but increase the total cost to develop and produce five landers by 1.70%. None of the costs in Fig. 5 include the cost of launching the lander from Earth or transporting it to Mars. That cost will depend on the design of the in-space propulsion stage which will be sized to the lander TMI mass. However, for previous missions the cost of delivering the vehicle to Mars was small compared to the cost of the lander hardware. For example, the Atlas V launch vehicle which launched MSL from Earth to its TMI orbit was only 17% the cost of the EDL vehicle[22]. Determining the effect of TMI mass on the total campaign cost is an important question but it is out of scope of this work.

The effects of lander payload and ballistic coefficient on the sizing of the aerocapture and EDL HIADs are shown in Figs. 5e and 5f. The tradespace covers a wide range of HIAD diameters ranging from 12 to 26 m. The cost and TMI mass differences in a lander with ballistic coefficient of 160 vs 120 kg/m^2 are explained by the difference in HIAD diameters. Changing the ballistic coefficient of a lander with 20 t payload from 160 to 120 requires increasing the aerocapture HIAD diameter by 2.4 m and the EDL HIAD diameter by 2.2 m. The increase in HIAD diameter significantly reduces the required propellant, which is inexpensive, but increases the area of the aerocapture HIAD by 65 m^2 and the area of the EDL HIAD by 56 m^2, which are much more costly.

For any human Mars campaign multiple landers will be required to deliver all the necessary equipment and provisions to the surface. Building a large number of smaller payload landers reduces the development cost, and production costs are reduced by producing multiple of the same unit. However, Fig. 5g shows that the cost per ton of payload is significantly reduced by increasing the payload per lander. Furthermore, Fig. 5j shows the gear ratio is also significantly reduced using landers with larger payloads. The gear ratio is the TMI mass divided by the payload mass and corresponds to the mass efficiency of the lander. A lower gear ratio means a higher percentage of the total mass sent to Mars is payload. Figures 5h and 5i show the total cost of lander hardware to deliver 100 t and 200 t of payload to the Martian surface. In each of these plots there are several local minimums and discontinuities. The discontinuities are a result of the how the landers are packed. For example, to deliver 100 t of payload it is very inefficient to design a lander with a 24 t payload capacity as five landers will need to be built each with 4 t of unused payload capacity. If instead 25 t payload landers are used, there will be no wasted capacity and only four landers need to be built. Figure 5h contains eight local minimums corresponding to the payloads that evenly divide 100. The most notable of these minimums are at 33.3, 25, 20, 16.7, and 14.3 t with the global minimum at 20 t. In Fig. 5i where the total payload to Mars has been doubled, the global minimum has shifted to 25 t. Figures 5k and 5l show the total TMI mass for campaigns sending 100 and 200 t to Mars, respectively. Again the local minimums are at lander payloads that evenly divide 100 and 200. However, unlike Figs. 5h and 5i the global minimums correspond to the maximum lander payload that evenly divides the campaign payload. The campaign payload is the total payload delivered to mars from several landers. These trends

are more clearly illustrated in Fig. 6.

Figure 6 includes every possible efficiently packed combination of landers, with individual payloads varying from 10-40 t, to deliver campaign payloads of 100, 150, 200, 250, or 300 t of to the surface of Mars. All costs in Fig. 6 are normalized to the first unit production cost of the baseline lander design.

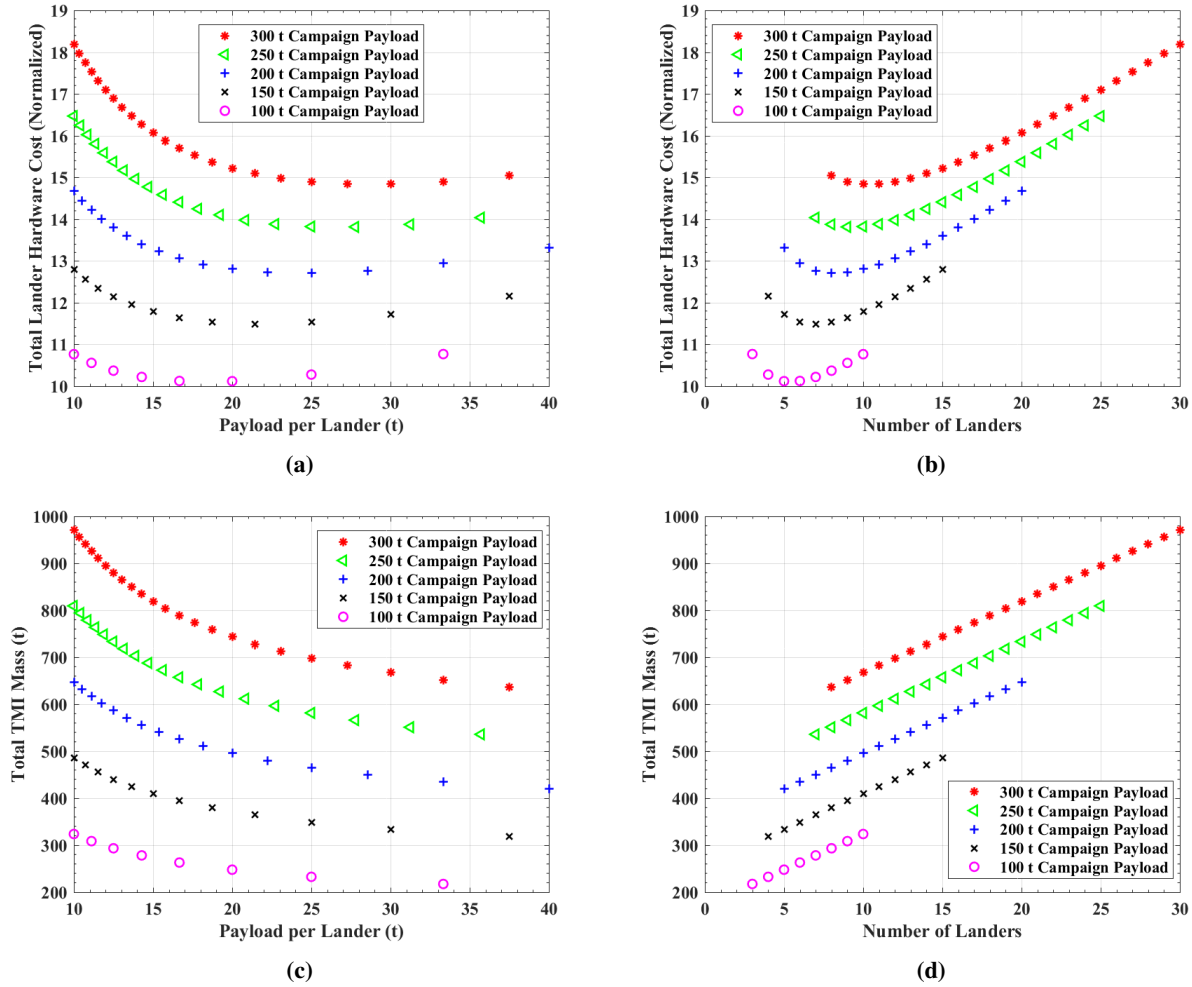

Fig. 6 Effects of lander payload on total cost and TMI mass for several possible multi-mission Mars campaigns.

Figures 6a and 6b show the total lander hardware costs as a function of payload per lander and number of landers. Note that for each campaign payload, increasing the payload per lander and decreasing the number of landers initially significantly reduces the total cost. As the payload per lander is increased further (and number of landers decreased) the total lander hardware cost reaches a minima and then increases. A slightly different trend is shown in Figs. 6c and 6d. Figures 6c and 6d show the total TMI mass over the campaign as a function of payload per lander and number of landers. In Figs. 6c and 6d as the payload per lander is increased (and number of landers decreased) the total TMI mass continuously decreases.

There are several important takeaways from Fig. 6.

1) Minimizing TMI mass does not always minimize lander hardware cost.
2) The TMI mass will always be minimized by maximizing the payload per lander and minimizing the number of landers.
3) Smaller lander designs are more cost effective for smaller campaigns sending less payload to Mars. Larger lander designs favor larger campaigns.
4) The majority of minimum cost lander designs have payloads between 20 and 30 t.
5) The total lander hardware cost is not very sensitive to the payload per lander in the vicinity of the minimum cost option. Meaning that there are many options for lander design that are not much more expensive than the minimum cost option. For example, 10 landers is the minimum cost option for a 300 t campaign, but the options sending 8-14 landers are all within 2% of the minimum cost option.
6) Larger campaigns are significantly more cost efficient. For example, sending 300 t to Mars only cost about 50 % more than sending 100 t.

Figure 7a shows the minimum cost payload per lander and number of landers for any campaign sending 40-800 t of payload to Mars. In other words Fig. 7a shows the what all minimum cost options from Figs. 6a and 6b would be if Figs. 6a and 6b included all campaigns from 40-800 t. The discontinuities in Fig. 7a represent where it is advantageous

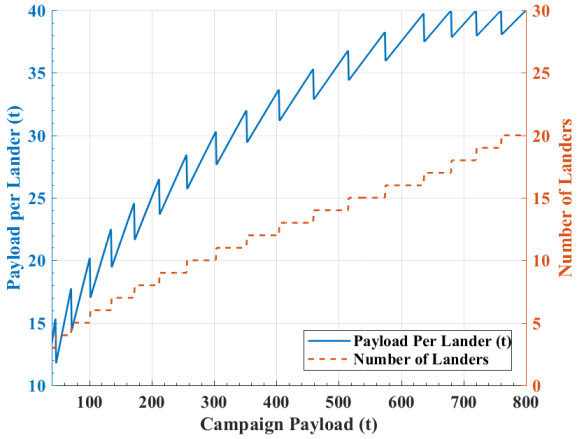

(a) Payload per lander and number of landers to minimize lander hardware costs over a campaign.

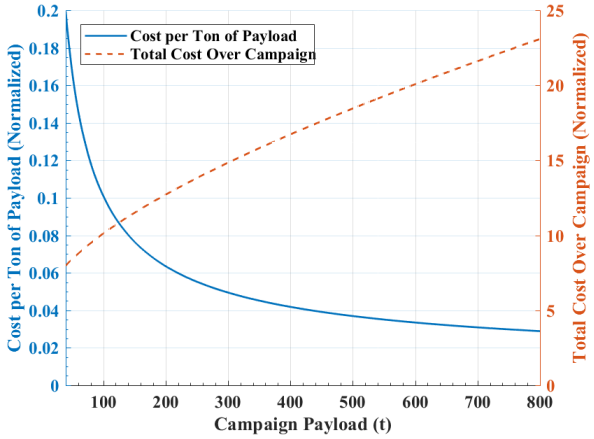

(b) Total lander hardware cost over campaign and hardware costs per ton of payload delivered.

Fig. 7 Considerations for a range of Mars campaign sizes.

to increase the number of landers by one and reduce the payload per lander accordingly. Figure. 7a also shows that there is no cost advantage to building landers with payloads over 40 t unless the campaign is sending over 720 t of payload to the surface. Figure 7b shows how the cost per ton of payload and the total lander hardware cost vary for campaigns sending 40-800 t of payload to Mars. Note that the cost of delivering one ton of payload to the surface drops

significantly as the total payload of the campaign increases. It also shows that the total cost associated with developing and building the lander hardware to deliver 800 t to the surface of Mars is only 23 times the first unit production cost of the baseline 20 t payload lander.

B. Payload vs. Ballistic Coefficient of Aerocapture HIAD

In Sec. IV.A the ballistic coefficient of both the aerocapture and EDL HIADs were varied but kept equal to each other. In this trade the Ballistic coefficient of the EDL HIAD is kept constant at 140 kg/m^2 while the aerocapture HIADs ballistic coefficient is varied from 100 to 180, and the payload capacity of the lander is varied from 10 to 40 t.

Figure 8 shows that in contrast to the results in Sec. IV.A both the cost and mass are minimized by maximizing the ballistic coefficient of the aerocapture HIAD. This makes intuitive sense as during aerocapture the main engines are not used so nothing material is gained or lost by changing the aerocapture HIAD diameter. At higher ballistic coefficients the vehicle must descend deeper in the Mars atmosphere and experiences a higher heat load. The increased heat load is mitigated by increasing the thickness of the flexible TPS. However, this work does not take into account after-body heating. The current models assume no backshell and only some light TPS at the rear of the spacecraft. Recent work has shown that radiative heating on the after-body of a spacecraft can be significant, exceed convective heating, and is highly dependent on angle of attack[23][24]. Since the vehicle is controlled by altering its angle of attack via trim tabs, after-body radiative heating could pose a significant risk to the payload if larger ballistic coefficients are used. As HIAD diameter decreases with higher ballistic coefficients, the risk of an infeasible lander design increases. Adding a backshell to mitigate this risk would be a significant added cost and operational problem. The backshell would have to be removed or open up for crew and cargo to be unloaded. Removing the backshell in flight requires a separation mechanism that ensures it does not recontact the lander or land on any assets already on the Martian surface. A backshell that opens up

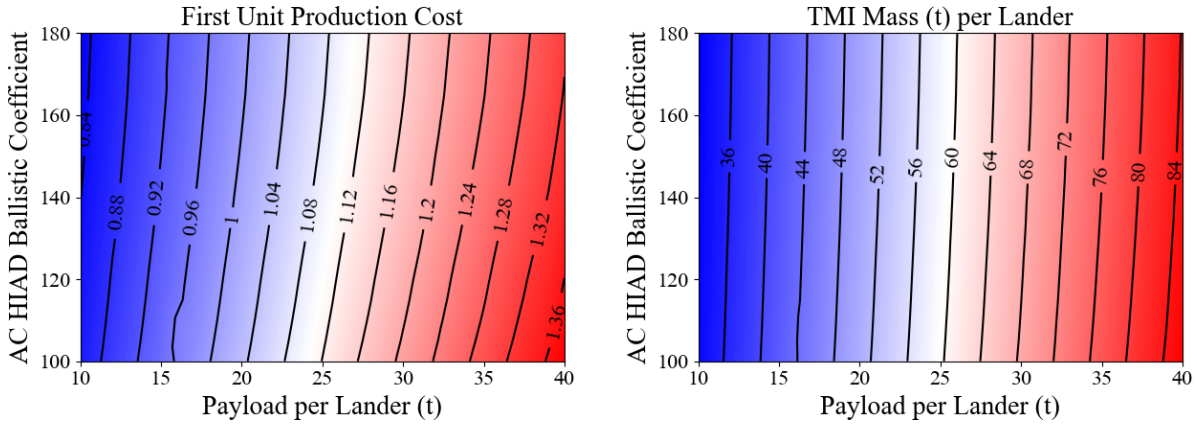

(a) **(b)**

Fig. 8 Lander payload and aerocapture HIAD ballistic coefficient tradespace.

once the lander has reached the surface will add mass to the vehicle and make offloading large cargo a challenge.

The complete set of SAPE-C output for the payload vs. aerocapture ballistic coefficient tradespace can be seen in Fig. 13 in the Appendix.

C. Payload vs. Ballistic Coefficient of EDL HIAD

In this trade the Ballistic coefficient of the aerocapture HIAD is kept constant at 140 kg/m^2 while the EDL HIAD ballistic coefficient is varied from 100 to 180 and the payload capacity of the lander is varied from 10 to 40 t. Figure 9a shows that the minimum cost configuration is when the EDL HIAD has a ballistic coefficient of 130 kg/m^2. However, Fig. 9a also shows that from ballistic coefficients of 105 to 150 kg/m^2 the cost varies less than 0.5%. Fig. 9b shows that for a given payload, the TMI mass continues to decrease as the ballistic coefficient decreases. Depending on how the

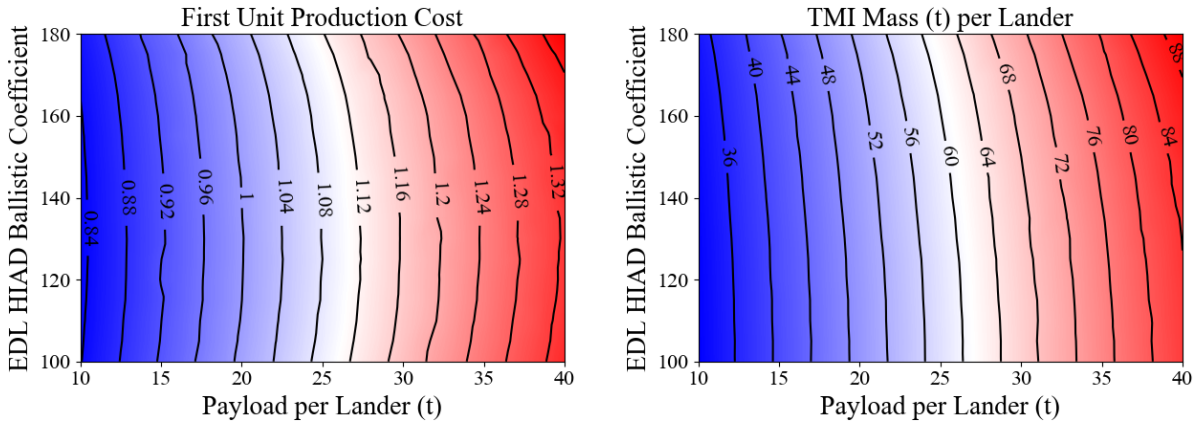

(a) **(b)**

Fig. 9 Lander payload and EDL HIAD ballistic coefficient tradespace.

cost of the in-space propulsion stage delivering the lander to TMI orbit varies with TMI mass, it may be more cost effective to build a lander with an EDL HIAD ballistic coefficient below 130 kg/m^2.

The complete set of SAPE-C output for the payload vs. EDL ballistic coefficient tradespace can be seen in Fig. 14 in the Appendix.

D. Payload vs. Specific Impulse

This tradespace examines the effect of the specific impulse of the landers eight main engines on lander cost and TMI mass. SEER does not have the capability to accurately estimate how changing the specific impulse of an engine will effect its cost. However, SAPE can size all other lander components as the propellant requirements change. Increasing the specific impulse of the main engines results in lower propellant mass, which in turn reduces the total mass of the lander as well as the mass and cost of the tanks, structures, thermal control systems, and several other subsystems. This trade does not take into account the additional costs or mass of improving the engines to operate at higher specific

impulses, only the effects on other lander subsystems.

Figure 10 shows the payload vs. specific impulse tradespace. The eight CH4-LOX main engines of the lander are assumed to have a nominal specific impulse of 360 s, which is varied ±10% from 324 to 396. Figure 10a shows an approximately linear decrease in cost as specific impulse increases. On average increasing specific impulse by 1% results in a 0.17% reduction in lander cost and a 0.22% decrease in TMI mass. Given the massive expense of a humans to Mars campaign, a 0.17% cost decrease is a considerable savings.

The complete set of SAPE-C output for the payload vs. specific impulse tradespace can be seen in Fig. 15 in the Appendix.

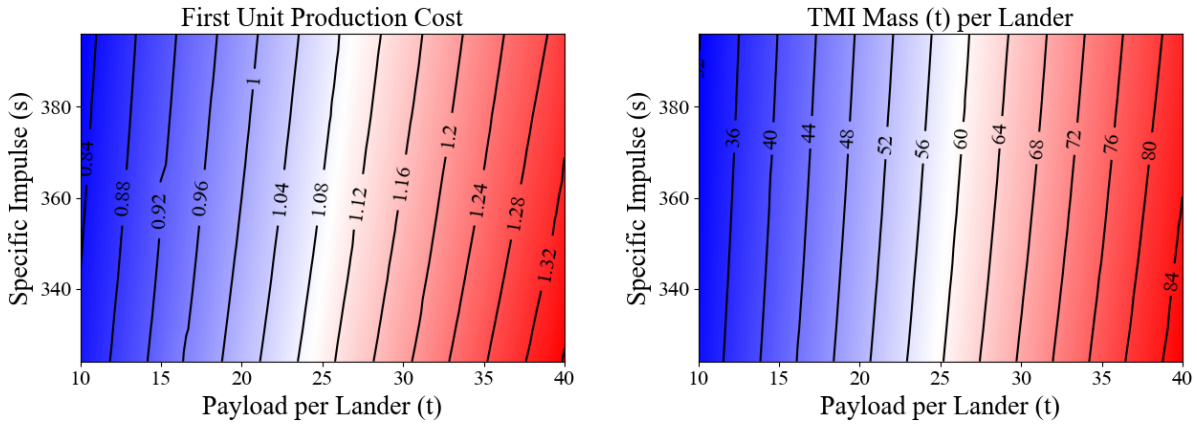

(a) **(b)**

Fig. 10 Lander payload and specific impulse tradespace.

E. Payload vs. Thrust-to-Weight Ratio

Increasing the thrust-to-weight ratio of the main engines allows the lander to come to a stop more quickly during its terminal descent phase and use less propellant, thereby reducing the required size of the propellant tanks, support structures, and cooling systems of the lander. The effect the thrust-to-weight ratio has on the cost and TMI mass is highly coupled as seen in Fig. 11.

Figure 11a shows that increasing the thrust-to-weight ratio above 1.5 is extremely beneficial. Increasing the Thrust-to-Weight ratio from 1.5 to 1.75 decreases the total production cost of the vehicle by 1.3%, and increasing it further to 2.0 decreases the production cost by 1.9%. However, increasing the thrust-to-weight ratio beyond 2.0 has diminishing returns. To get a 3% decrease in cost, the thrust-to-weight ratio must be increased to 2.75. Increasing the thrust-to-weight ratio to 4.0 only achieves a 3.6% cost reduction. It should be noted that at this point SAPE-C does not model the effect of engine thrust on the cost of the landers engine. The cost reductions seen here will have to be balanced against the additional cost and mass of larger more powerful engines.

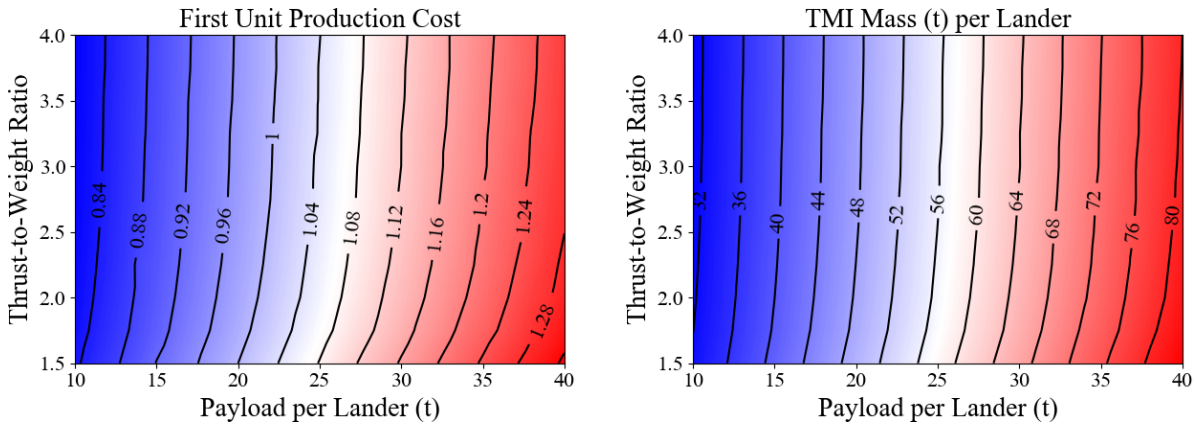

(a) **(b)**

Fig. 11 Lander payload and thrust-to-weight ratio tradespace.

The complete set of SAPE-C output for the payload vs. thrust-to-weight ratio tradespace can be seen in Fig. 16 in the Appendix.

V. Uncertainty Quantification Capabilities of SAPE-C

The goal of this section is to demonstrate the uncertainty quantification capabilities of SAPE-C. With any space mission it is essentially impossible to predict the cost with complete accuracy because of the many sources of uncertainty. A primary source of uncertainty in the preliminary design phase of a mission is the uncertainty in the mass of the spacecraft and each of its components. In the present work, uncertainty in the mission cost due to uncertainty in the mass of the spacecraft's components is refereed to as "mass uncertainty." Many other sources of uncertainty in the cost of a space mission are intangible items which are difficult to quantify such as delays in funding, political hurdles, volatility of goals and requirements, uncertainty in the maturity of a technology, or prolonged launch delays due to any number of external factors. These kinds of uncertainties are refereed to as "mission uncertainties."

While it is impossible to accurately predict the exact cost of a space mission, it may be possible to accurately predict the distribution of possible costs with uncertainty analysis. As stated previously, SEER outputs the values of a CDF at 10% intervals. Thus, the range from the 10% probability level to the 90% probability level is the 80% Confidence Interval (CI). In a previous study by Friz et al., the CIs obtained with SEER have been validated for different space missions.[18].

SAPE-C can output an absolute CI and a relative CI. The absolute CI, C_a is defined as

$$C_a = x_{90} - x_{10} \tag{2}$$

where x_{90} is the cost estimate at the 90% confidence level, and x_{10} is the cost estimate at the 10% confidence level. The relative CI, C_r, is defined as

$$C_r = \frac{x_{90} - x_{10}}{x_{50}} \tag{3}$$

where x_{50} is the cost estimate at the 50% confidence level which was also used as the point estimates presented in Sec. IV.

Figure 12 shows the absolute and relative CIs of the first unit production cost for the baseline lander design as payload and ballistic coefficient are varied. Figures 12a and 12b show the uncertainty in cost due only to the uncertainty in the mass modeling, while Figs. 12c and 12d show the uncertainty in cost due to all mission factors. Both the mass and mission CI follow the same trend as the first unit production cost seen in Fig 5b. As the mass of the payload per lander increases so does the first unit production cost and the first unit production cost CI. Similarly, both the first unit production cost and its CI are minimized at ballistic coefficients near 160 kg/m^2. However, the relative confidence

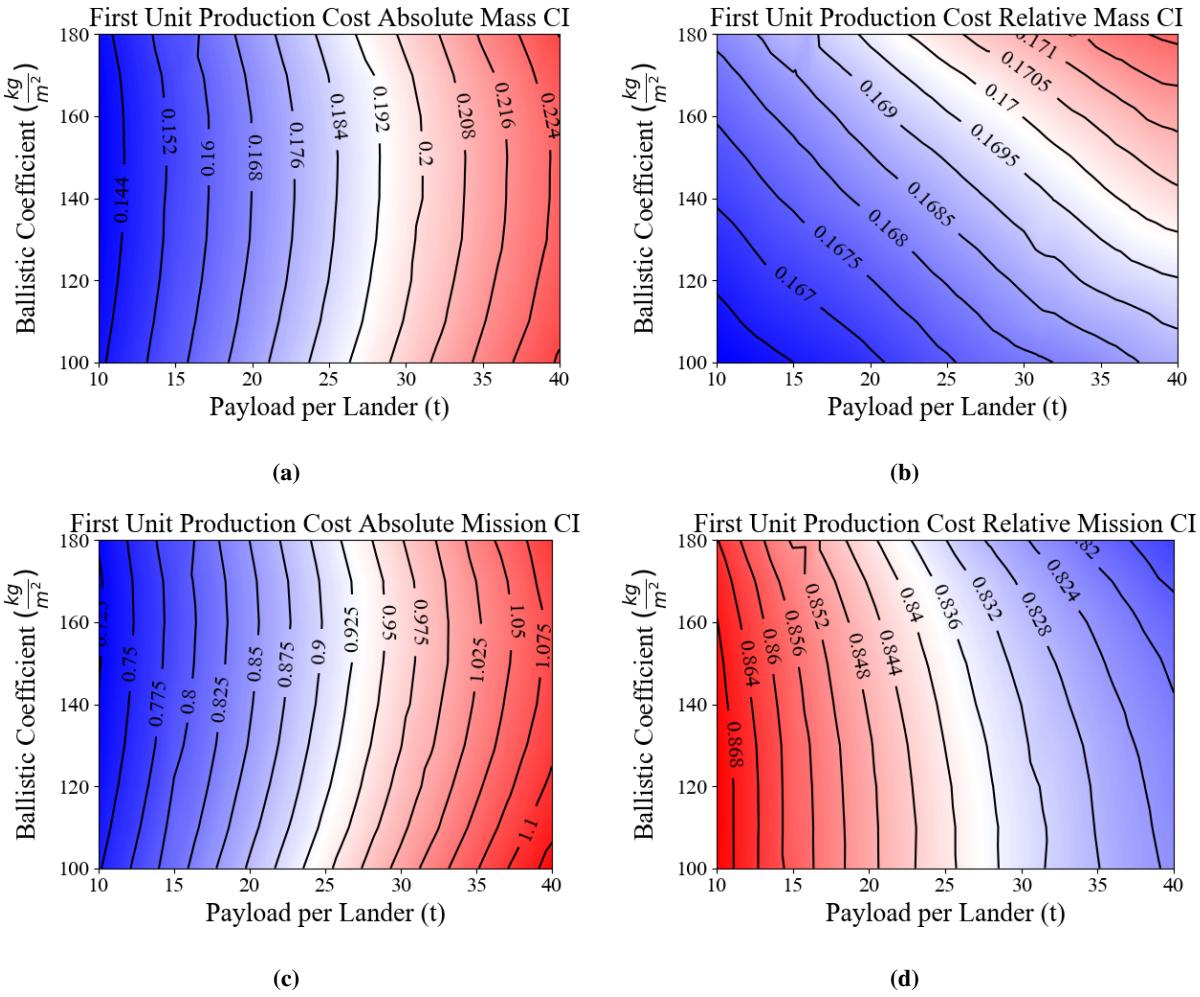

Fig. 12 Uncertainty for the payload vs ballistic coefficient tradespace.

interval follows a much different trend. Overall the relative CI does not vary significantly with ballistic coefficient or payload. The total variation in Fig.12b is about 2 % and in Fig. 12d is less than 6%. These variations are an order of magnitude smaller than the variations seen in Figs. 12a and 12c. Interestingly, the relative mission CI does decrease slightly with increasing payload, which is opposite of the absolute CI trend. However, the major take away from comparing relative and absolute uncertainty is that while the absolute uncertainty increases as lander payload increases the relative uncertainty does not, meaning there is no additional cost risk associated with larger payload landers.

VI. Conclusions

SAPE-C, the new extension to the systems analysis tool SAPE was presented. SAPE-C allows the user to quickly determine the effect that an improved technology or change in vehicle configuration will have on the cost of an entire vehicle. By linking the output of several systems analysis tools with the commercial cost estimating software SEER, SAPE-C is able to model costs in a dynamic way not possible with traditional costing tools. This work used SAPE-C to explore the effects of payload, ballistic coefficients, main engine specific impulse, and main engine thrust-to-weight ratio on the total hardware cost of a HIAD entry vehicle.

It was determined that lander hardware costs are not minimized by minimizing the TMI mass. Payload per lander is the factor which has the largest impact on lander hardware costs over a campaign. Designing a lander to carry more payload decreases its gear ratio making it more mass efficient, in addition the first unit production cost per ton of payload also decreases. However, this also increases the development cost and reduces the cost efficiency of building multiple identical units. The payload per lander that minimizes lander hardware costs is dependent upon the total payload being delivered to Mars, and trends to higher payloads per lander as the total campaign payload increases. In contrast, to minimize TMI mass, the payload per lander should be made as large as possible.

The cost of a lander with a given payload can be minimized by designing the ballistic coefficient of the aerocapture HIAD to be as large as possible without requiring a backshell or putting the vehicle at risk. In contrast, a large EDL HIAD with a smaller ballistic coefficient can reduce propulsion requirements and costs. Costs are minimized when the EDL HIAD's ballistic coefficient is around 130 kg/m^2. Decreasing the ballistic coefficient of the EDL HIAD below 130 kg/m^2 will increase the cost of the lander hardware but also decrease the TMI mass.

Specific impulse also has a significant effect on cost. For every 1% that specific impulse is raised, it reduces lander costs by 0.17% and TMI mass by 0.22%. Improving CH4-LOX engines to increase specific impulse will reduce costs as long as the cost of improving the engines and extra mass from extending nozzles does not outweigh the cost and mass savings. Increasing engine thrust to allow a higher thrust-to-weight ratio can also reduce cost. However, this study was not able to determine the thrust-to-weight ratio that minimized cost as SAPE-C is currently not modeling how a number of key propulsion components are changing with thrust.

In this paper, the uncertainty quantification capabilities of SAPE-C were also demonstrated. SAPE-C is capable of

generating at Confidence Interval (CI) for each estimate in the tradespace. It was determined that while the size of the CIs increase as the payload of the lander increases the CI relative to an estimates median cost stays fairly constant.

The primary item for future work is modeling the effect of TMI mass on the mission cost. To model the effect of TMI mass on campaign cost would require modeling a propulsion stage in both EXAMINE and SEER where the prime input to the vehicle sizing would be TMI mass. Ideally several propulsion concepts would be modeled and compared so that the effect of the propulsion technology on the cost can also be studied. Reducing the total TMI mass across the campaign by increasing lander payload and HIAD diameters will reduce the cost of transporting the landers to Mars but may not reduce the total campaign costs. As the cost of access to space continues to decreases so will the benefit of reducing TMI mass.

Appendix: Complete SAPE-C Output

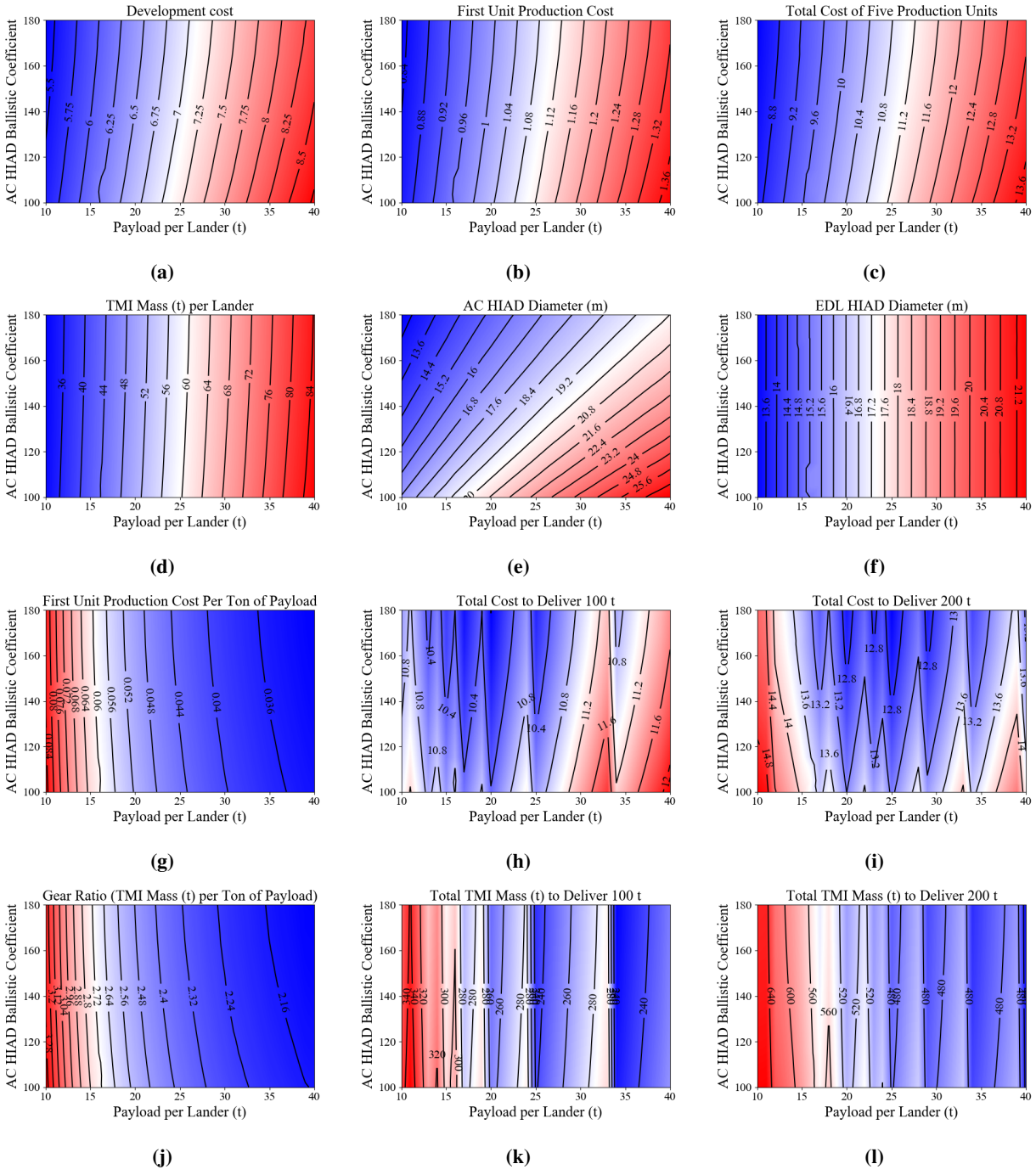

Fig. 13 Payload vs. Aerocapture HIAD Ballistic Coefficient Trades.

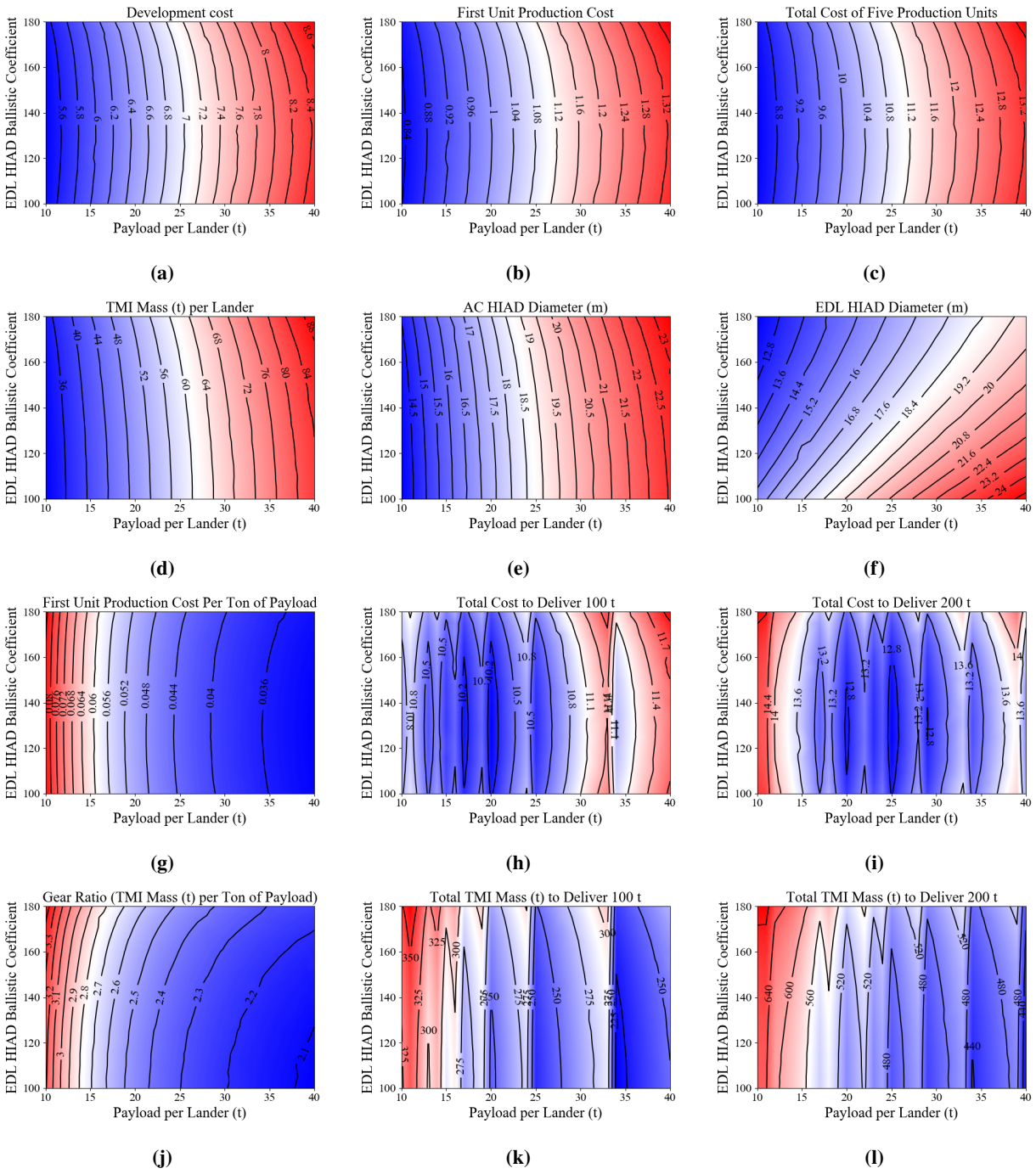

Fig. 14 Payload vs. EDL HIAD Ballistic Coefficient Trades.

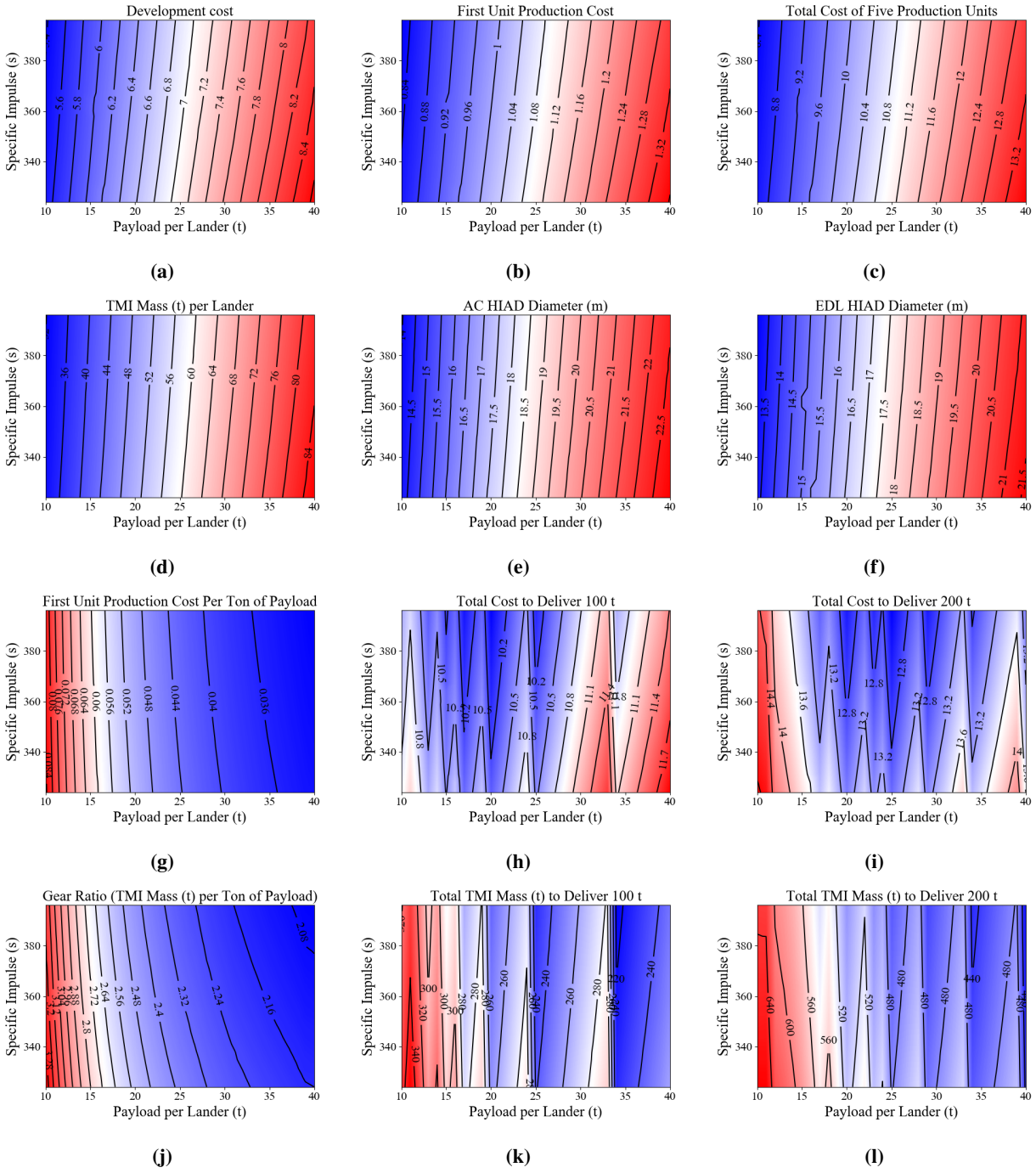

Fig. 15 Payload vs. Specific Impulse Trades.

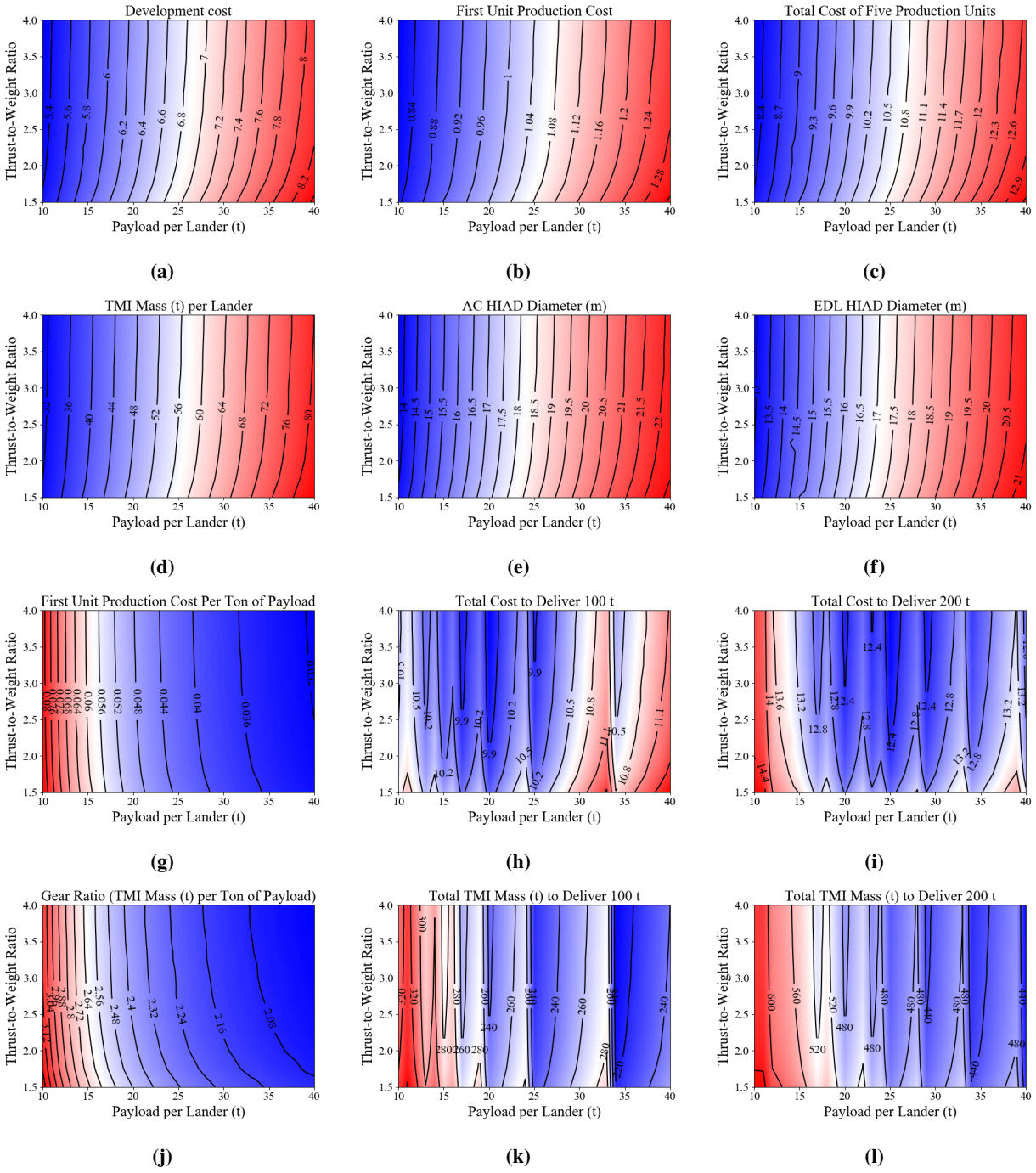

Fig. 16 Payload vs. Thrust-to-Weight Ratio Trades.

References

[1] Rapp, D., "Human Missions to Mars: Enabling Technologies For Exploring the Red Planet," 2016.

[2] Portree, D. S., "Humans to Mars: Fifty Years of Mission Planning, 1950-2000," 2001.

[3] Drake, B. G., "Mars Human Exploration Mission DRA 5.0," Tech. rep., NASA-SP-2009-566, July, 2009.

[4] Samareh, J. A., "A Multidisciplinary Tool for Systems Analysis of Planetary Entry, Descent, and Landing (SAPE)," Tech. rep., NASA/TM-2009-215950, L-19730, LF99-9217, 2009.

[5] Samareh, J., Glaab, L., Winski, R. G., Maddock, R. W., Emmett, A. L., Munk, M. M., Agrawal, P., Sepka, S., Aliaga, J., Zarchi, K., et al., "Multi-Mission System Analysis for Planetary Entry (M-SAPE) Version 1," Tech. rep., NASA/TM2014-218507, L-20440, NF1676L-19269, 2014.

[6] Bruce III, W. E., Mesick, N. J., Ferlemann, P. G., Siemers III, P. M., DelCorso, J. A., Hughes, S. J., Tobin, S. A., and Kardell, M. P., "Aerothermal ground testing of flexible thermal protection systems for hypersonic inflatable aerodynamic decelerators," *9th International Planetary Probe Workshop*, 2012.

[7] Dillman, R., Hughes, S., DiNonno, J., Bodkin, R., White, J., DelCorso, J., and Cheatwood, F., "Planned Flight of the Terrestrial HIAD Orbital Reentry (THOR)," 2014.

[8] Li, L., Gonyea, K., and Braun, R. D., "Finite Element Analysis of the Inflatable Re-Entry Vehicle Experiment (IRVE)," *56th AIAA/ASCE/AHS/ASC Structures, Structural Dynamics, and Materials Conference*, 2015, p. 0204. doi:10.2514/6.2015-0204, URL https://doi.org/10.2514/6.2015-0204.

[9] Brown, G., Epp, C., Graves, C., Lingard, S., Darley, M., and Jordan, K., "Hypercone inflatable supersonic decelerator," *17th AIAA Aerodynamic Decelerator Systems Technology Conference and Seminar*, 2003, p. 2167.

[10] Langston, S., Lang, C. G., Daryabeigi, K., and Samareh, J., "Optimization of a Hot Structure Aeroshell and Nose Cap for Mars Atmospheric Entry," *AIAA SPACE 2016*, 2016, p. 5594. doi:10.2514/6.2016-5594, URL https://doi.org/10.2514/6.2016-5594.

[11] Gnoffo, P. A., and Cheatwood, F. M., "User's manual for the Langley aerothermodynamic upwind relaxation algorithm (LAURA)," 1996.

[12] Johnston, C. O., Gnoffo, P. A., and Sutton, K., "Influence of ablation on radiative heating for earth entry," *Journal of Spacecraft and Rockets*, Vol. 46, No. 3, 2009, pp. 481–491.

[13] Johnston, C. O., Hollis, B. R., and Sutton, K., "Spectrum modeling for air shock-layer radiation at lunar-return conditions," *Journal of Spacecraft and Rockets*, Vol. 45, No. 5, 2008, pp. 865–878.

[14] Johnston, C. O., Hollis, B. R., and Sutton, K., "Non-Boltzmann modeling for air shock-layer radiation at lunar-return conditions," *Journal of Spacecraft and Rockets*, Vol. 45, No. 5, 2008, pp. 879–890.

[15] Komar, D., Hoffman, J., Olds, A., and Seal, M., "Framework for the Parametric System Modeling of Space Exploration Architectures," *AIAA Space 2008 Conference & Exposition*, 2008, p. 7845.

[16] Brauer, G., Cornick, D., and Stevenson, R., "Capabilities and applications of the Program to Optimize Simulated Trajectories (POST). Program summary document," 1977.

[17] Sanchez, S., and Kha, K., "SEER Validation Study Results for NASA Space Science Missions," , 2015.

[18] Friz, P. D., Klovstad, J. J., Leser, B. B., Towle, B. C., and Hosder, S., "Blind Study Validating Parametric Costing Tools Price TruePlanning and SEER-H for NASA Science Missions," *21st AIAA Space Conference*, 2018.

[19] Galorath, "SEER-H Space Guidance: Revision 2.2," , 2016.

[20] Yarnell, N., "Design, verification/validation and operations principles for flight systems," *Jet Propulsion Laboratory, D-17868, Rev 1*, Vol. 2, 2003.

[21] Lillard, R., and Olejniczak, J., "Human Mars EDL pathfinder study: Assessment of technology development gaps and mitigations," *Aerospace Conference, 2017 IEEE*, IEEE, 2017, pp. 1–8.

[22] Spagnuolo, J., "Mars Science Laboratory Cost Analysis Data Requirement (CADRe) Launch," , 2011.

[23] Brandis, A. M., Cruden, B. A., White, T. R., Saunders, D. A., and Johnston, C. O., "Radiative heating on the after-body of Martian entry vehicles," *45th AIAA Thermophysics Conference*, 2015, p. 3111.

[24] West, T. K., Theisinger, J., Brune, A. J., and Johnston, C. O., "Backshell Radiative Heating on Human-Scale Mars Entry Vehicles," *47th AIAA Thermophysics Conference*, 2017, p. 4532.